AIP | Journal of Applied Physics

Effects of high temperature annealing on single crystal ZnO and ZnO devices

W. Mtangi, F. D. Auret, M. Diale, W. E. Meyer, A. Chawanda et al.

Citation: J. Appl. Phys. **111**, 084503 (2012); doi: 10.1063/1.3700186
View online: http://dx.doi.org/10.1063/1.3700186
View Table of Contents: http://jap.aip.org/resource/1/JAPIAU/v111/i8
Published by the American Institute of Physics.

Related Articles

Theoretical study of Si-based ionic switch
Appl. Phys. Lett. 100, 203506 (2012)

AlN thin film transducers for high temperature non-destructive testing applications
J. Appl. Phys. 111, 074510 (2012)

Fast programming metal-gate Si quantum dot nonvolatile memory using green nanosecond laser spike annealing
Appl. Phys. Lett. 100, 143501 (2012)

Al2O3/InAs metal-oxide-semiconductor capacitors on (100) and (111)B substrates
Appl. Phys. Lett. 100, 132905 (2012)

Sub-diffraction-limit semiconductor resonators operating on the fundamental magnetic resonance
Appl. Phys. Lett. 100, 131113 (2012)

Additional information on J. Appl. Phys.

Journal Homepage: http://jap.aip.org/
Journal Information: http://jap.aip.org/about/about_the_journal
Top downloads: http://jap.aip.org/features/most_downloaded
Information for Authors: http://jap.aip.org/authors

ADVERTISEMENT

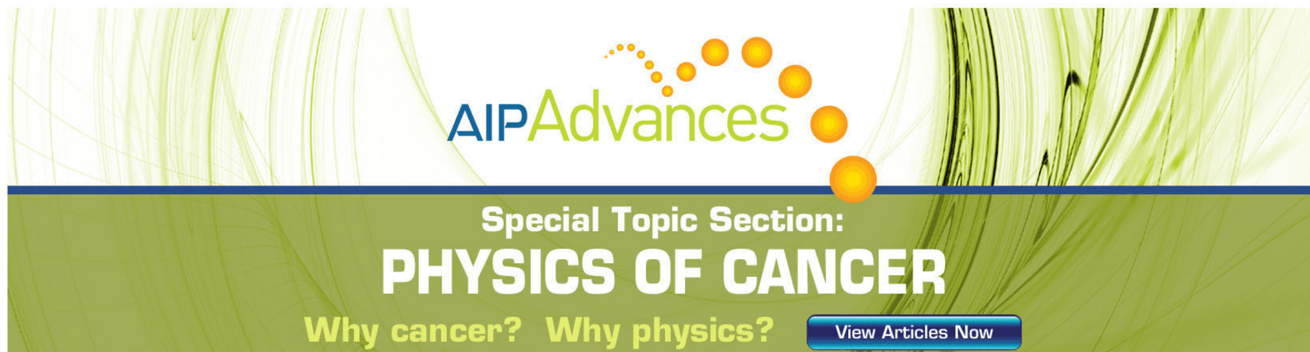

Downloaded 05 Jun 2012 to 137.215.6.53. Redistribution subject to AIP license or copyright; see http://jap.aip.org/about/rights_and_permissions

Effects of high temperature annealing on single crystal ZnO and ZnO devices

W. Mtangi, F. D. Auret, M. Diale, W. E. Meyer, A. Chawanda, H. de Meyer, P. J. Janse van Rensburg, and J. M. Nel
Department of Physics, University of Pretoria, Private Bag X20, Hatfield 0028, South Africa

(Received 17 January 2012; accepted 2 March 2012; published online 16 April 2012)

We have systematically investigated the effects of high-temperature annealing on ZnO and ZnO devices using current voltage, deep level transient spectroscopy (DLTS) and Laplace DLTS measurements. Current–voltage measurements reveal the decrease in the quality of devices fabricated on the annealed samples, with the high-temperature annealed samples yielding devices with low barrier heights and high reverse currents. DLTS results indicate the presence of three prominent defects in the as-received samples. Annealing the ZnO samples at 300 °C, 500 °C, and 600 °C in Ar results in an increase in reverse leakage current of the Schottky contacts and an introduction of a new broad peak. After 700 °C annealing, the broad peak is no longer present, but a new defect with an activation enthalpy of 0.18 eV is observed. Further annealing of the samples in oxygen after Ar annealing causes an increase in intensity of the broad peak. High-resolution Laplace DLTS has been successfully employed to resolve the closely spaced energy levels. © *2012 American Institute of Physics*. [http://dx.doi.org/10.1063/1.3700186]

INTRODUCTION

ZnO is a wide and direct bandgap semiconductor with experimental bandgap energy of 3.4 eV. Its high exciton binding energy of 60 meV at room temperature and resistance to radiation damage gives it advantages and makes it a good candidate for fabrication of devices that can operate within the ultraviolet region and space applications compared to other wide bandgap materials, e.g., GaN. ZnO exists mostly as n-type, whose conductivity is supposedly due to the existence of native point defects, such as oxygen vacancies and Zn interstitials.[1,2] Some other impurities, such as hydrogen, are also claimed to contribute to the n-type conductivity in ZnO.[3–5] As in many wide bandgap semiconductors, there exists a so-called doping asymmetry,[6] i.e., it is easy to get n-type ZnO, but rather difficult to produce p-type ZnO. The use of ZnO in the optoelectronic industry for fabrication of high performance solar cells and ultraviolet detectors requires the material to be of high quality, i.e., with minimal defects. The knowledge of the origins, identity, quality, and stability of defects in ZnO is of vital importance, as defects often affect the electrical and optical properties of the material. Defects can also reduce device lifetime and decrease the light emission efficiency.[6] The existence of native defects in ZnO has hindered success in the fabrication of UV-emitting diodes, because of their self-compensation behavior.[7,3] ZnO also possesses deep-level emission bands that emit all colors in the visible range with good color-rendering properties.[8] An understanding of the origins of emissions related to deep-level defects in ZnO for development of high efficiency optoelectronic devices is also required. There is a need to have control over the conductivity and defects in ZnO, i.e., by removing them if unwanted or introducing them when required. Annealing of crystals is one possible way of recovering defects or removing them. The study of defects in ZnO through annealing has been performed using the Hall effect,[9–11] positron annihilation spectroscopy,[12] x ray diffraction, Rutherford backscattering spectroscopy (RBS), admittance spectroscopy,[13] cathodoluminescence, and photoluminescence.[14] In this paper, we study the effects of annealing on ZnO and the electrical properties of the devices formed on the annealed material. The quality of the devices fabricated on the annealed samples is characterized using IV measurements, while deep level transient spectroscopy and Laplace DLTS are used to study the deep-level defects introduced in the annealed material.

EXPERIMENT

Single-crystal ZnO samples obtained from Cermet Inc. were used in this study. In this experiment, five sets consisting of two samples per set with the same specifications were used. All the sets were annealed in argon ambient for 1 h at different temperatures. The first set was annealed at 300 °C, the second set at 400 °C, the third set at 500 °C, the fourth set at 600 °C, and the fifth set at 700 °C. A sample from the same as-received wafers was also used as the control. One sample from each annealed set was used for the fabrication of Schottky contacts in the first part of the experiment. Prior to Schottky contact and ohmic contact fabrication, the annealed and control samples were degreased in acetone followed by methanol for five minutes in an ultrasonic bath. The five-minute degrease in methanol was followed by a three-minute boiling in hydrogen peroxide at a temperature of 100 °C. The samples were then blown dry using nitrogen gas. Al/Au ohmic contacts were then fabricated on the O-polar face using the thermal evaporation technique. Pd Schottky contacts with a diameter of 0.6 mm were then fabricated on the Zn-polar face using the resistive evaporation technique to ensure that no process-induced defects were introduced into the material, as has been reported.[15] In the second part of the experiment, the remaining samples from each set were each annealed at the same temperature at which they were annealed before, but this time in oxygen

 © 2012 American Institute of Physics

Downloaded 05 Jun 2012 to 137.215.6.53. Redistribution subject to AIP license or copyright; see http://jap.aip.org/about/rights_and_permissions

ambient. The cleaning of the samples was the same as the one outlined in the first part of the experiment. Pd Schottky contacts and Al/Au ohmic contacts with the same thicknesses were then fabricated, as in the first part. Current-voltage measurements were then performed in the dark at a temperature of 296 K. DLTS and Laplace DLTS measurements were finally performed to characterize the defects induced by annealing ZnO single crystals.

RESULTS AND DISCUSSIONS

Figure 1(a) shows the semi-logarithmic IV characteristics obtained from the Schottky contacts fabricated on the Ar-annealed and un-annealed samples, while Fig. 1(b) shows the IV characteristics obtained on the Ar and then O_2-annealed samples. From these characteristics, it can be observed that the annealed samples produce contacts with high reverse currents compared to the un-annealed sample. The quality of the contacts deteriorates after annealing the Ar-annealed samples further in O_2. Of particular interest is the leakage current that has been obtained on the 400 °C- and 500 °C-annealed samples. This is possibly due to the effects of annealing and the defects introduced in the material. This is going to be discussed in detail in the sections to follow. The IV characteristics of the contacts have been analyzed by fitting the linear part of the forward IV characteristics to the pure thermionic emission model.

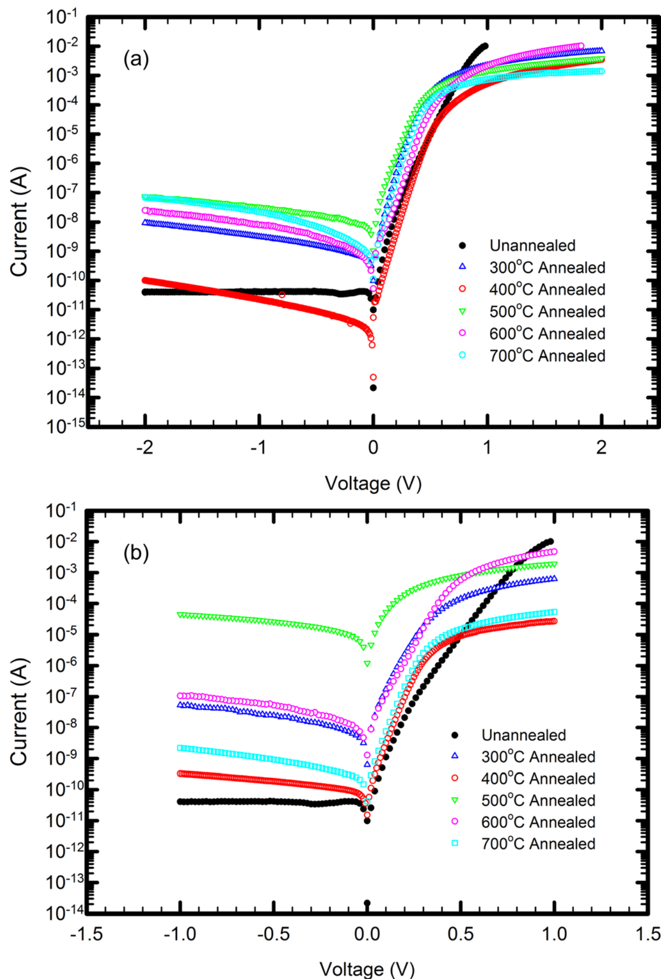

FIG. 1. (a) IV characteristics for the Ar-annealed samples obtained at 296 K. (b) IV characteristics for the Ar + O_2-annealed samples obtained at 296 K.

TABLE I. Values of Schottky barrier height (*SBH*), ideality factor *n*, and series resistance R_s for the Ar and Ar + O_2-annealed for the best selected contacts.

Annealing temperature (°C)	SBH (eV)		Ideality factor		Series resistance (Ω)	
	Ar	Ar + O_2	Ar	Ar + O_2	Ar	Ar + O_2
300	0.70	0.64	1.25	1.45	206	936
400	0.81	0.75	1.37	1.15	312	29k
500	0.63	0.48	1.72	1.54	391	411
600	0.74	0.64	1.43	1.55	110	100
700	0.73	0.74	1.17	1.14	8.4k	12k
Un-annealed	0.74		1.67		190	

Table I shows the parameters that were obtained from the IV characteristics of Figs. 1(a) and 1(b). The 500 °C-annealed samples reveal the lowest barrier heights after annealing in Ar and also Ar and then O_2. High barrier heights have been measured for the 400 °C-annealed samples. There has been an increase in series resistance after Ar and then O_2 annealing for all the other temperatures examined. This could possibly be due to the formation of an insulative oxide layer that might have been formed during oxygen annealing.

Figures 2(a) and 2(b) show the DLTS spectra for the Ar-annealed and Ar- and then O_2-annealed samples, respectively. These spectra were obtained in the 30–330-K temperature range, at a reverse bias of –2.0 V, filling pulse width of 2.0 ms, and filling pulse of 0.3 V. The annealed samples and the un-annealed samples show three prominent defects, E1, E2, and E3, that have been observed in ZnO and reported before.[16–19] The 300 °C Ar annealing of the ZnO samples introduces a new peak $E4_{300\,°C}$, as has also been reported by Ref. 20. After annealing at 400 °C, no new peak is introduced, but only the intensity of E1 increases. After 500 °C annealing, a broad peak $E4_{500\,°C}$ is also observed. A broad peak $E4_{600\,°C}$ is also observed after 600 °C annealing. After 700 °C annealing, $E4_T$ is not observed, but a new peak Ex is observed. (N.B.: T refers to the annealing temperature at which the peak is introduced). The formation of new defects affects the IV characteristics and parameters of the Schottky contacts. As has been mentioned before, the 400 °C-annealed samples have very low leakage current and high barrier heights, since there are no new defects introduced. It can be stated that the defects introduced in ZnO are the cause of high leakage currents and low barrier heights, as they modify the current transport mechanisms by which carriers crossover the barrier. These mechanisms could include all forms of tunneling through the barrier.

We have annealed the Ar annealed samples in oxygen ambient in a bid to see if the Ar annealing-induced defects could be removed by oxygen annealing. This is because, in our previous results,[20] we have observed that oxygen annealing does not introduce E4. From Fig. 2(b), it can be clearly seen that Ar annealing followed by O_2 annealing does not

Downloaded 05 Jun 2012 to 137.215.6.53. Redistribution subject to AIP license or copyright; see http://jap.aip.org/about/rights_and_permissions

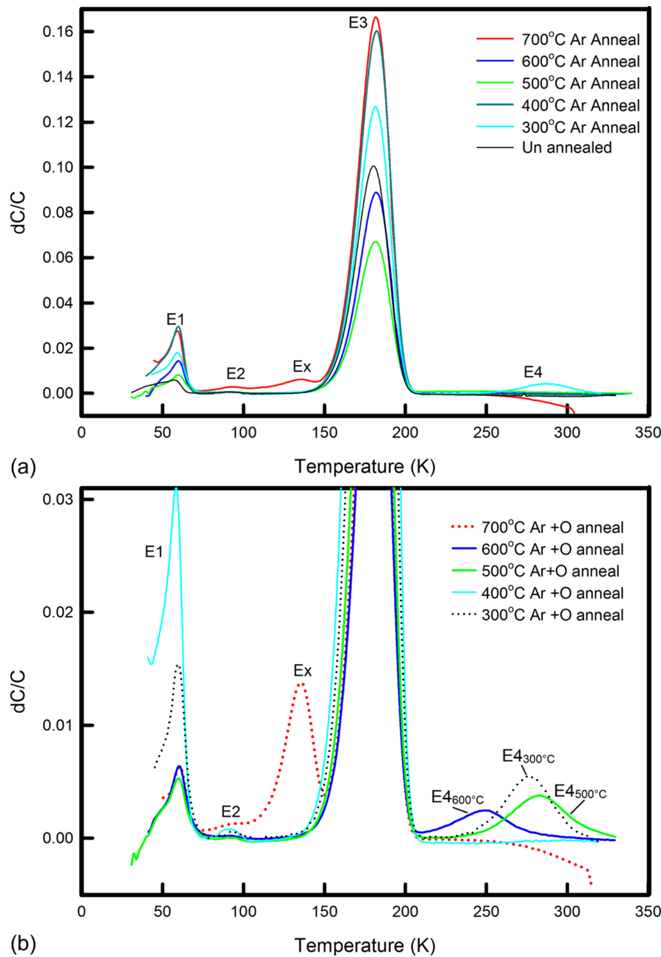

FIG. 2. (a) DLTS spectra obtained from the Ar-annealed samples at a quiescent reverse bias of 2.0 V, $V_p = 0.3$ V, filling pulse width of 2 ms, and rate window of 100 s^{-1}. (b) DLTS spectra obtained from the Ar + O_2-annealed samples at a quiescent reverse bias of 2.0 V, $V_p = 0.3$ V, filling pulse width of 2 ms, and rate window of 100 s^{-1}.

remove $E4_T$, but rather causes an increase in the intensity of $E4_T$ and Ex. This means that, once $E4_T$ has been introduced, it is difficult to anneal it out at the same temperature at which it forms. The $E4_T$ peak is very broad, indicating that it might consist of two or more closely spaced energy levels.

Figure 3 shows the Arrhenius plots for the E1, E2, Ex, and E3 defects. The identities of E1 = E_c – 0.12 denotes that E1 is located at an energy level of 0.12 eV below the minimum of the conduction band. The same applies to E2 and E3. E1 = E_c – 0.12, E2 = E_c – 0.10, and E3 = E_c – 0.30 are still not clear, though others have tried to identify them using their annealing behaviors to O_i or V_{zn}; for E1,[20] transition metal related; for E3.[19] Ex has been estimated to have an activation enthalpy of 0.18 eV. Its identity is not known yet.

High-resolution Laplace DLTS[21,22] has been employed to separate the closely spaced energy levels in the E4 peak in the Ar- and then O_2-annealed samples. Figure 4(a) shows the Laplace spectra for the 300 °C-annealed sample. Laplace has managed to split $E4_{300\,°C}$ into three peaks. The Arrhenius plots are given in Fig. 4(b). Figure 5(a) shows the Laplace spectra for the 500 °C-annealed samples, whose Arrhenius plots are given in Fig. 5(b). Figure 6(a) shows the Laplace spectra obtained from the 600 °C-annealed

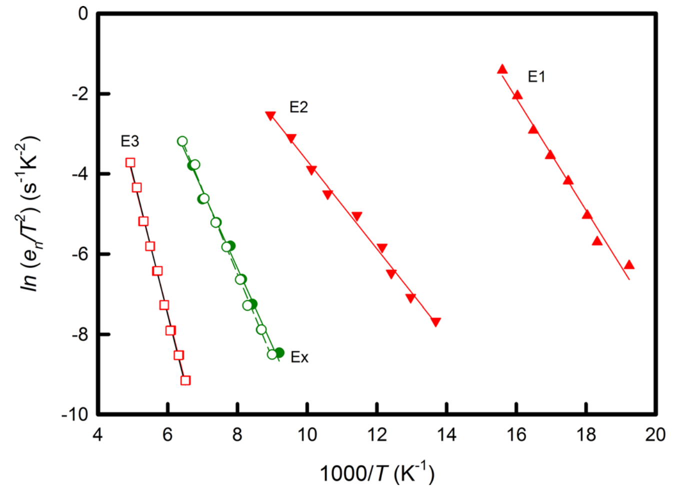

FIG. 3. Arrhenius plots obtained from the Ar-annealed samples.

samples, and the Arrhenius plots are presented in Fig. 6(b). The 600 °C-annealed samples have only two peaks. The associated energy levels and apparent capture cross sections are presented in Table II. It must be noted that the annealing-induced defect at 300 °C might not be the same as the one introduced at 500 °C and also 600 °C. The

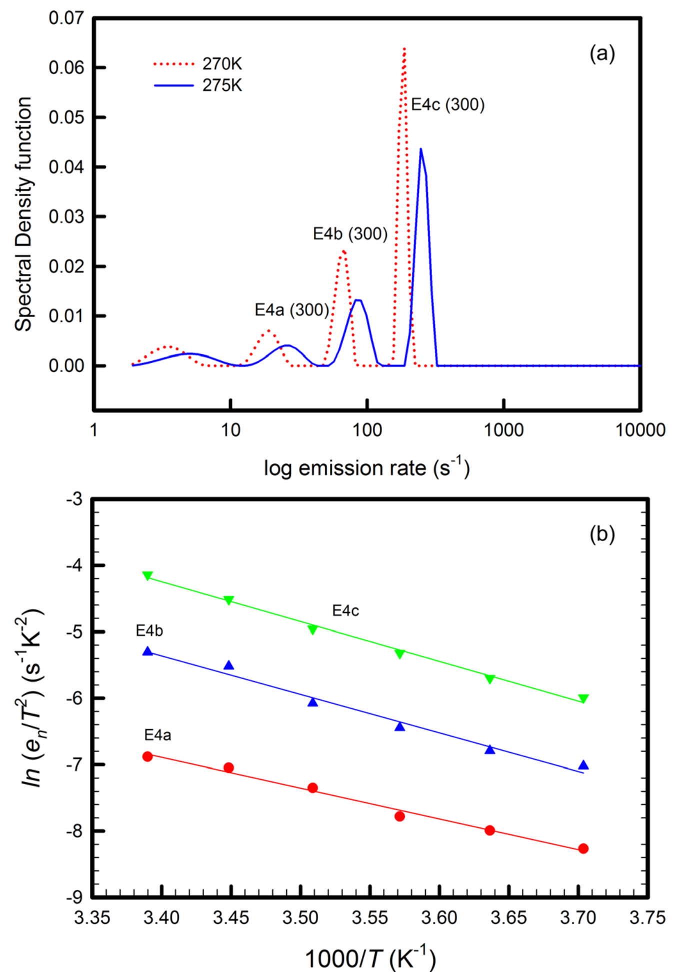

FIG. 4. (a) Laplace DLTS spectra obtained from the 300 °C Ar + O_2-annealed samples. These were measured at a reverse bias of 2.0 V, filling pulse height of 0.30 V, and width of 2 ms. (b) Arrhenius plots obtained from the 300 °C Ar + O_2-annealed samples.

Downloaded 05 Jun 2012 to 137.215.6.53. Redistribution subject to AIP license or copyright; see http://jap.aip.org/about/rights_and_permissions

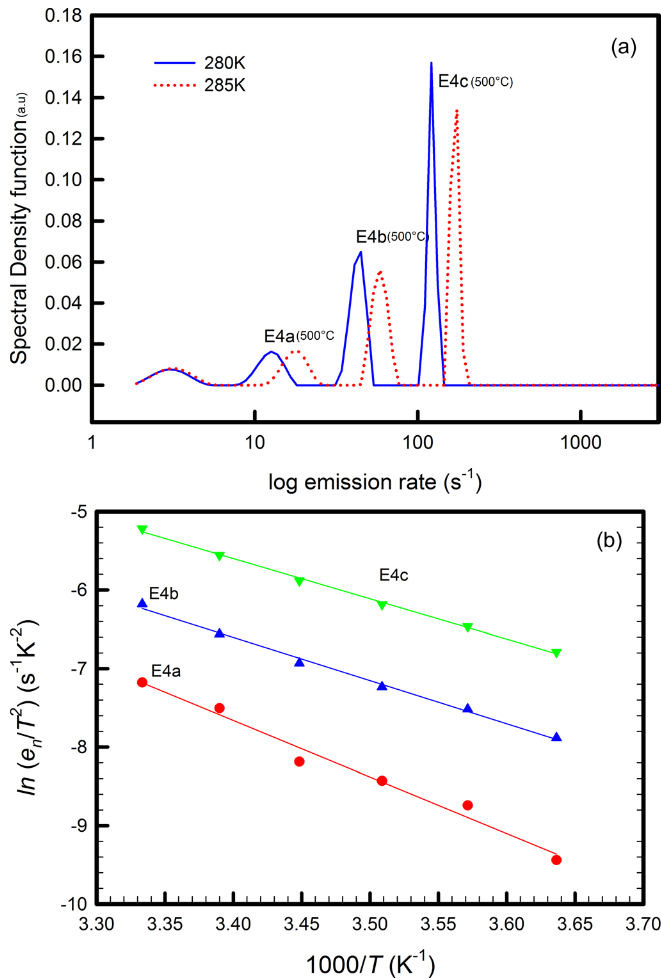

FIG. 5. (a) Laplace DLTS spectra obtained from the 500 °C Ar + O_2-annealed samples. These were measured at a reverse bias of 2.0 V, filling pulse height of 0.30 V, and width of 2 ms. (b) Arrhenius plots obtained from the 500 °C Ar + O_2-annealed samples.

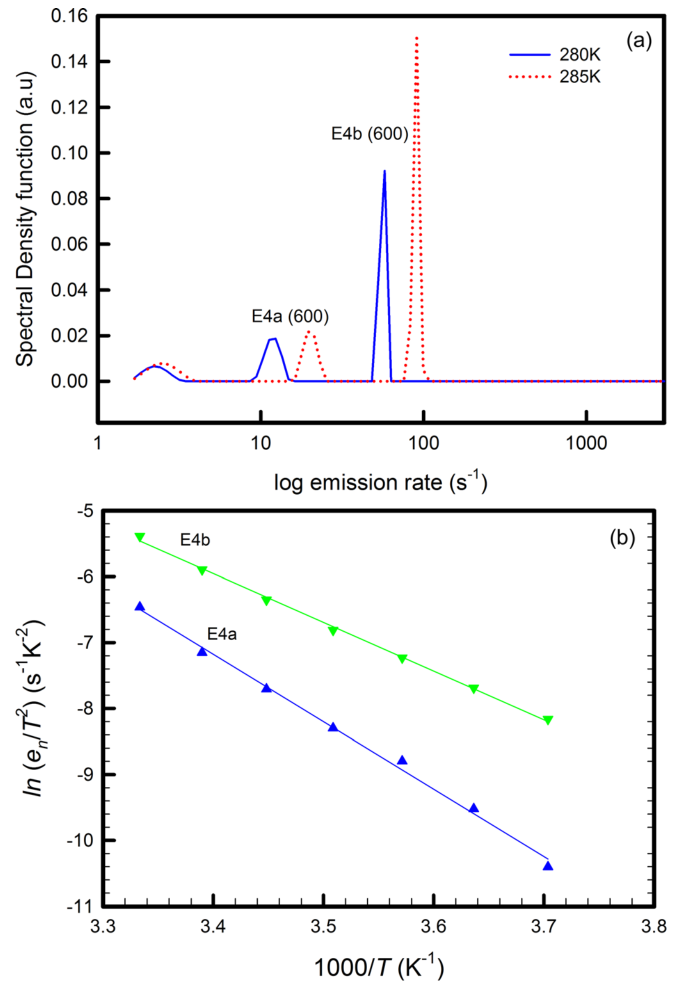

FIG. 6. (a) Laplace DLTS spectra obtained from the 600 °C Ar + O_2-annealed samples. These were measured at a reverse bias of 2.0 V, filling pulse height of 0.30 V, and width of 2 ms. (b) Arrhenius plots obtained from the 600 °C Ar + O_2-annealed samples.

difference in the activation enthalpy and capture cross-sectional area of the annealing-induced defects for different annealing temperatures indicates the possible transformation of defects with annealing. The 300 °C-induced defect appears to be neutral, judging from its small capture cross-section. Since, at 400 °C, the defect is not observed, it can be mentioned that it is mobile at a temperature greater than 300 °C, but less than 400 °C. This is in close agreement with the first principles calculations of Janotti *et al.*,[23] which suggest that the V_o^{2+} anneals out at a temperature of 655 K. This annealing out of a defect at 400 °C was also observed by Vlasenko and Watkins[24] from the Optically Detected Electron Paramagnetic resonance measurements, where they reported the stability of the L3 peak up to a temperature of 400 °C, after which it disappears.

The physical meaning of the capture cross-sections of the 500 °C-annealed and 600 °C-annealed contacts is not clear yet. From the Laplace Arrhenius plots of the 500 °C-annealed samples, E4a has an apparent capture cross section, which might suggest it to be an intermediate defect. The 600 °C anneal produces a defect whose capture cross-section is too large. This value of the capture cross-section is too large to have any physical meaning. The error in this value is

TABLE II. Values of energy level and apparent capture cross section for the E4 defect observed after Ar + O_2 annealing, obtained using Laplace DLTS.

	E4a (T[a])		E4b (T[a])		E4c (T[a])	
Annealing temperature (°C)	Energy level (eV)	Capture cross section (cm^2)	Energy level (eV)	Capture cross section (cm^2)	Energy level (eV)	Capture cross section (cm^2)
300	0.49	3.9e−15	0.52	6.4e−14	0.53	2.3e−13
500	0.62	3.0e−13	0.47	2.8e−15	0.44	2.1e−15
600	0.88	1.5e−8	0.64	3.2e−12		

[a]T denotes the temperature at which the sample was annealed.

Downloaded 05 Jun 2012 to 137.215.6.53. Redistribution subject to AIP license or copyright; see http://jap.aip.org/about/rights_and_permissions

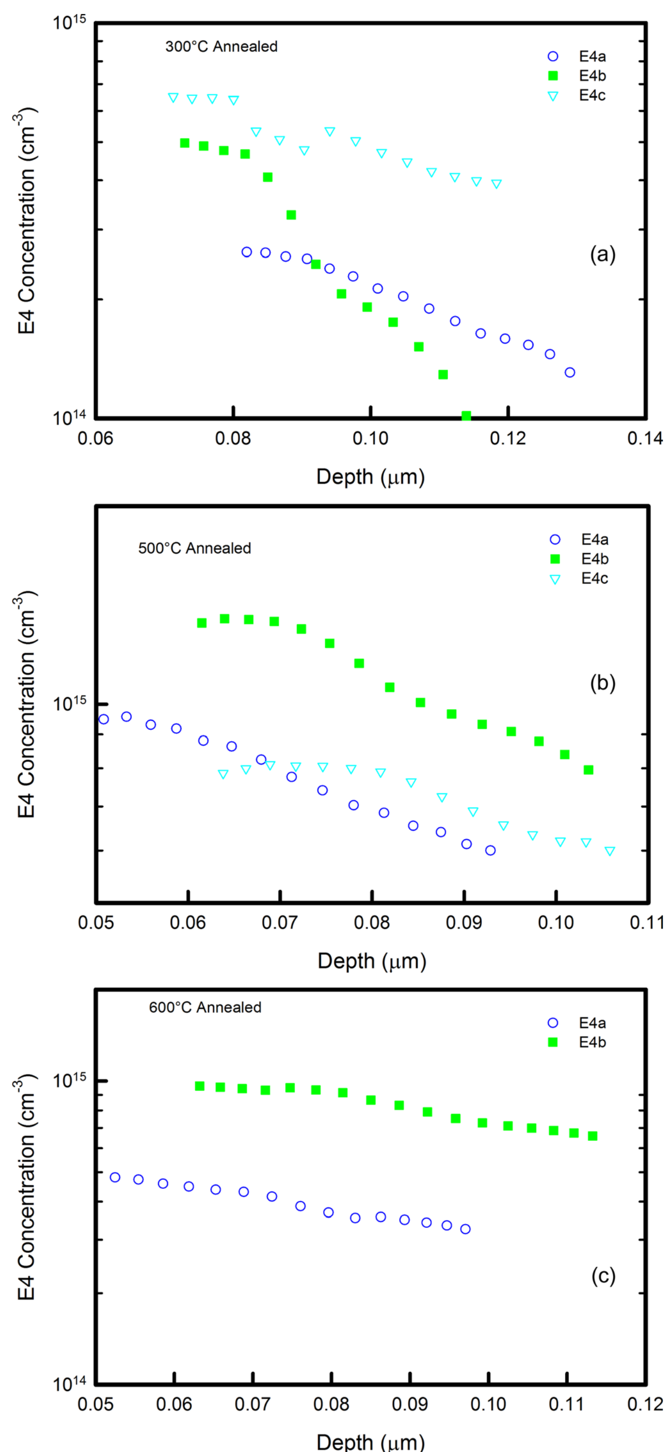

FIG. 7. (a) Depth profile obtained from the 300 °C Ar + O_2-annealed samples. This was determined at a constant reverse bias of 2.0 V with increasing filling pulse height in steps of 0.1 V. (b) Depth profile obtained from the 500 °C Ar + O_2-annealed samples. This was determined at a constant reverse bias of 2.0 V with increasing filling pulse height in steps of 0.1 V. (c) Depth profile obtained from the 600 °C Ar + O_2-annealed samples. This was determined at a constant reverse bias of 2.0 V with increasing filling pulse height in steps of 0.1 V.

$\pm 8 \times 10^{-9}$cm^2. Further investigations have to be performed to try and understand the reasons behind this large value. At a temperature between 600 °C and 700 °C, this defect anneals out, as it is not observed at 700 °C. This defect might possibly be related to the V_o^0. This is because the V_o^0 anneals out at a temperature of 909 K,[23] which falls within the 600 °C to 700 °C temperature range.

Figures 7(a)–7(c) show the depth profiles of the components of the $E4_T$ peak for the ZnO samples annealed in Ar and then O_2 at 300 °C, 500 °C, and 600 °C, respectively. This has been obtained at a constant reverse bias of –2.0 V and increasing pulses in steps of 0.1 V. From the variation of the trap concentration with depth, i.e., a decrease in concentration as we move from the interface into the ZnO bulk, it can clearly be observed that annealing of ZnO creates defects whose concentration decreases as we move deeper into the semiconductor bulk. Similar observations have been noted and reported from the Hall effect measurements.[25]

CONCLUSION

As-received ZnO has three prominent defects, which are native to the material, as observed using conventional DLTS. Deep-level defects in ZnO can be recovered by annealing the material at high temperatures in Ar ambient. The 300 °C, 500 °C, and 600 °C Ar annealings introduce a broad peak consisting of energy levels which are closely spaced and can be separated by the high-resolution Laplace DLTS. Annealing single-crystal ZnO samples at 400 °C in Ar does not introduce a new defect, but causes an increase in intensity of the E1 peak. The 700 °C annealing does not introduce the $E4_T$, but rather introduces a level closer to the minimum of the conduction band, Ex with an activation enthalpy of 0.18 eV. Further annealing of the samples in O_2 causes an increase in intensity of the annealing-induced defect peaks. From the IV characteristics of the devices fabricated on the as-received and annealed samples, it can be observed that the annealed samples yield poor quality devices, i.e., with high reverse currents and low barrier heights compared to the as-received samples. Annealing single crystal ZnO samples at high temperatures introduces defects with high concentrations closer to the metal/semiconductor interface that affect device operation by modifying the current transport mechanism from pure thermionic emission to other mechanisms that include all forms of tunneling.

ACKNOWLEDGMENTS

We would like to thank the South African National Research Foundation (NRF) for financial support. The Laplace DLTS software and hardware used in the research was kindly provided by A. R. Peaker (Centre for Electronic Materials Devices and Nanostructures, University of Manchester) and L. Dobaczewski (Institute of Physics, Polish Academy of Sciences).

[1]Y. Natsume and H. Sakata, Mater. Chem. Phys. **78**, 170, (2002).
[2]D. C. Look, J. W. Hemsky, and J. R. Sizelove, Phys. Rev. Lett. **82**, 2552, (1999).
[3]F. A. Selim, M. H. Weber, D. Solodovnikov, and K. G. Lynn, "Nature of native defects in ZnO," Phys. Rev. Lett. **99**, 085502 (2007).
[4]C. G. Van de Walle, Phys. Rev. Lett. **85**, 1012, (2000).
[5]D. M. Hofmann *et al.*, Phys. Rev. Lett. **88**, 045504 (2002).
[6]Z. Q. Chen, S. Yamamoto, M. Maekawa, A. Kawasuso, X. L. Yuan, and T. Sekiguchi, J. Appl. Phys. **94**(8), 4807 (2003).
[7]Y. Tsur and I. Riess, Phys. Rev. B **60**, 8138 (1999).

Downloaded 05 Jun 2012 to 137.215.6.53. Redistribution subject to AIP license or copyright; see http://jap.aip.org/about/rights_and_permissions

[8]N. H. Alvi, K. ul Hasan, O. Nur, and M. Willander, Nanoscale Res. Lett. **6**, 130 (2011).
[9]W. Mtangi, J. M. Nel, F. D. Auret, A. Chawanda, M. Diale, and C. Nyamhere, "Annealing and surface conduction on Hydrogen peroxide treated bulk melt-grown, single crystal ZnO," Physica B **407**, 1624 (2012).
[10]G. H. Kassier, M. Hayes, F. D. Auret, M. Diale, and B. G. Svensson, Phys. Status Solidi C **5**, 569 (2008).
[11]D. C. Look, Superlattices Microstruct. **42**, 284 (2007).
[12]D. Sanyal, T. K. Roy, M. Chakrabarti, S. Dechoudhury, D. Bhowmick, and A. Chakrabarti, J. Phys.: Condens. Matter **20**, 045217 (2008).
[13]D. Seghier and H. P. Gislason, J. Mater. Sci.: Mater. Electron. **19**, 687 (2008).
[14]D. C. Look, G. C. Farlow, P. Reunchan, S. Limpijumnong, S. B. Zhang, and K. Nordlund, Phys. Rev. Lett. **95**, 225502 (2005).
[15]W. Mtangi, F. D. Auret, P. J. Janse van Rensburg, S. M. M. Coelho, M. J. Legodi, J. M. Nel, W. E. Meyer, and A. Chawanda, J. Appl. Phys. **110**, 094504 (2011).
[16]F. D. Auret, S. A. Goodman, M. Hayes, M. J. Legodi, H. A. van Laarhoven, and D. C. Look, J. Phys.: Condens. Matter **13**, 8989 (2001).
[17]M. Grundmann, H. v. Wenckstern, R. Pickenhain, Th. Nobis, A. Rahm, and M. Lorenz, Superlattices Microstruct. **38**, 317 (2005).
[18]A. Y. Polyakov, N. B. Smirnov, E. A. Kozhukhova, V. I. Vdovin, K. Ip, Y. W. Heo, D. P. Norton, and S. J. Pearton, Appl. Phys. Lett. **83**, 1575 (2003).
[19]H. von Wenckstern, G. Biehne, M. Lorenz, M. Grundmann, F. D. Auret, W. E. Meyer, P. J. Janse van Rensburg, M. Hayes, and J. M. Nel, J. Korean Phys. Soc. **53**, 2861 (2008).
[20]W. Mtangi, F. D. Auret *et al.*, Effects of hydrogen, oxygen and argon annealing on the electrical properties of ZnO and ZnO devices studied by Current-voltage, deep level transient spectroscopy (DLTS) and Laplace DLTS J. Appl. Phys. (submitted).
[21]L. Dobaczewski, P. Kaczor, I. D. Hawkins, and A. R Peaker, J. Appl. Phys. **76**, 194 (1994).
[22]L. Dobaczewski, A. R Peaker, and K. Bonde Nielsen, J. Appl. Phys. **96**, 4689 (2004).
[23]A. Janotti and C. G. van de Walle, Phys. Rev. B **76**, 165202 (2007).
[24]L. S. Vlasenko and G. D. Watkins, Phys. Rev. B **71**, 125210 (2005).
[25]D. C. Look, B. Claflin, and H. E. Smith, Appl. Phys. Lett. **92**, 122108 (2008).

Downloaded 05 Jun 2012 to 137.215.6.53. Redistribution subject to AIP license or copyright; see http://jap.aip.org/about/rights_and_permissions